Novel anti-cancer agents based on germacrone: design, synthesis, biological activity, docking studies and MD simulations†

Lianbao Ye,*[a] Jie Wu,[a] Weiqiang Chen,[b] Yu Feng[a] and Zhibing Shen[c]

Germacrone is a major activity component found in *Curcuma zedoaria* oil product, which is extracted from *Curcuma zedoaria*. In the present study, novel germacrone derivatives were first designed based on the theories of bioalkylating agents, synthesized, and then investigated for their inhibition effects on Bel-7402, HepG2, A549, and HeLa cells. Moreover, the study also evaluated the inhibition of these derivatives on c-Met kinase, which is expressed in a number of cancers. The results indicated that most of the compounds showed a stronger inhibitory effect on cancer cells and c-Met kinase than germacrone. Besides these findings, molecular docking studies were also carried out to analyze the results and explain the molecular mechanism of activities to c-Met kinase. Molecular dynamics simulations have been carried out for the further evaluation of binding stabilities between the compounds and their receptors.

Introduction

Curcuma zedoaria (Christm.) Roscoe, also called zedoary, is a common plant grown in tropical countries and it is used as a natural flavor, spice, and herb in Indonesia, India, and China. In China, it is traditionally used for the treatment of dyspepsia, menstrual disorders, flatulence, fever, and cough.[1,2] *Curcuma zedoaria* extract exhibit antitumor, antimicrobial, analgesic, and anti-allergic activities.[3–6] Germacrone is a major activity component found in zedoary oil product, which is extracted from *Curcuma zedoaria*. Germacrone (Fig. 1) has various kinds of biological activities, including antiulcer, anti-bacterial, anti-fungal, antitumor, antitussive, antifeedant, depressant, anti-inflammatory, hepatoprotector, vasodilator, and choleretic effects.[7–10]

The overexpression and mutation of c-Met and its natural ligand, hepatocyte growth factor (HGF), have been found in different types of tumors including colorectal, lung, pancreatic, breast, gastric, prostate, ovarian, head and neck, glioma, hepatocellular, renal, melanoma, and a number of sarcomas; this overexpression and mutation is correlated with advanced stays and poor prognosis.[11–13] Activation of the HGF/c-Met signaling pathway has been shown to lead to a wide array of

cellular responses including proliferation, angiogenesis, survival, tissue regeneration, wound healing, scattering, motility, branching morphogenesis and invasion.[14–17] Therefore, c-Met has become an attractive target for anti-tumor therapy.

Sulfonates have been widely used as anticancer drugs. In the alkylation reaction of organic synthesis, the existence of the sulfonate group can make the C–O bond active and become a useful alkylation reaction reagent.[18] Based on the design theories of bioalkylating agents and combination principles, different sulfonate esters at C-8 were introduced on germacrone to obtain novel derivatives 3a–3f (Fig. 2). These compounds might form intermediates with electrophilic groups and react with the rich electron groups of biomacromolecules (such as DNA, RNA or some important enzymes) to form the covalent binding *in vivo* resulting in the loss of activity of the DNA molecule, thus playing the role of an antitumor agent.[18]

In this study, we prepared these compounds and evaluated their inhibitions on Bel-7402, HepG2, A549, and HeLa cells. Simultaneously, the study evaluated the inhibition of these derivatives on c-Met kinase, which has been overexpressed in a number of cancers. Further, molecular docking studies
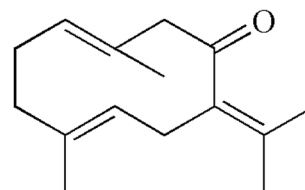
[a]Medicinal Chemistry of Department, Guangdong Pharmaceutical University, Guangzhou 510006, China. E-mail: yelb7909@163.com; Fax: +86-20-39352129; Tel: +86-20-39352139

[b]School of Basic Courses, Guangdong Pharmaceutical University, Guangzhou 510006, China

[c]School of Traditional Chinese Medicine, Guangdong Pharmaceutical University, Guangzhou, Guangdong, 510006, China

Fig. 1 Structure of germacrone.

Paper

Fig. 2 Germacrone derivatives.

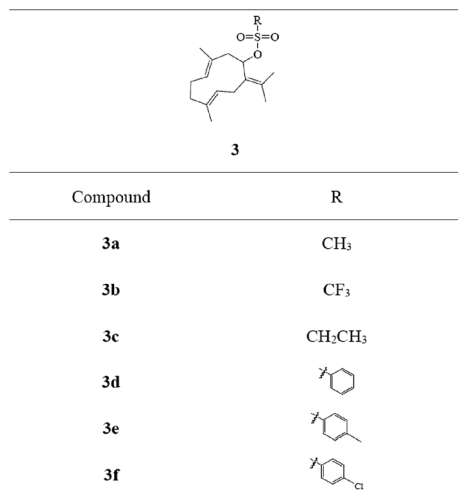| Compound	R
3a	CH₃
3b	CF₃
3c	CH₂CH₃
3d	(phenyl)
3e	(4-methylphenyl)
3f	(4-chlorophenyl)

analyzed the results and explained the molecular mechanism of eminent activities to c-Met kinase. Molecular dynamics simulations were applied to carry out further evaluation of the binding stabilities between compounds and their receptors.

Materials and methods

All chemicals were purchased from Aladdin or J&K Scientific Ltd. China. Germacrone (99.99%) was obtained from Chengdu Push Bio-technology Co., Ltd. Solvents were purified and dried based on standard procedures and stored over 3 Å molecular sieves. Reactions were tested by TLC using SILG/UV 254 silica-gel plates. Flash chromatography (FC) was carried out by silica gel column chromatography. ^{1}H NMR and ^{13}C NMR spectra were obtained using a Bruker Digital NMR Spectrometer, rep. δ in ppm, J in Hz. EI-MS was obtained using a Waters ZQ4000 instrument. Cells were obtained from the China Center for Type Culture Collection of Wuhan University; c-Met kinase was purchased from Millipore (Billerica, MA). RPMI-1640 culture medium and new-born calf serum were purchased from Gibco (Grand Island, NY), and methyl thiazolyl tetrazolium (MTT) was purchased from Amresco (Solon, OH).

Synthesis of compounds

Synthesis of 2. A suspension of LiAlH₄ (3.8 mg, 0.1 mmol) was added to a cold (−10 °C) solution of **1** (21.8 mg, 0.1 mmol) in THF (15 mL) under argon and vigorous stirring. After 1 h (TLC control), the reaction was terminated by the addition of water (2 drops), 6 N NaOH solution (2 drops), and water (4 drops). The mixture was extracted with DCM (3 × 20 mL) to obtain a crude product, which was purified by column chromatography (hexane/t-butyl methyl ether, 70/30) to obtain **2** (18.3 mg, 84%).

Synthesis of 3a. A mixture of methanesulfonic acid (14.4 mg, 0.15 mmol), SOCl₂ (21.4 mg, 0.18 mmol), DMF (2 drops), and DCM (5 mL) was refluxed for 4 h to obtain methanesulfonyl chloride. Methanesulfonyl chloride (17.1 mg, 0.15 mmol) was

added portion wise to a solution of **2** (21.9 mg, 0.1 mmol), pyridine (15.8 mg, 0.2 mmol) in THF (15 mL) at 0 °C under nitrogen. Then, the mixture was stirred for 4 h at r.t. (TLC control) and the solution was filtered. The solvent was removed and the crude product was purified by column chromatography (ethyl/acetate, 80/20) to obtain **3a** (19.9 mg, 67%).

Synthesis of 3b, 3c, and 3d. Compounds **3b**, **3c**, and **3d** were prepared in analogy to **3a**.

Synthesis of 3e. A mixture of **2** (21.9 mg, 0.1 mmol), DMAP (6.1 mg, 0.05 mmol), toluene-4-sulfonic acid (17.2 mg, 0.1 mmol), and DCM (10 mL) was stirred for 30 min under nitrogen at −10 °C. A solution of DCC (41.2 mg, 0.2 mmol) in DCM (5 mL) was slowly added and the mixture was vigorously stirred for 24 h at r.t. and filtered. The solvent was removed to give a crude product, which was purified by column chromatography to obtain the product **3e** (23.1 mg, 62%).

Synthesis of 3f. Compound **3f** was prepared in analogy to **3e**.

(3E,7E)-3,7-Dimethyl-10-(propan-2-ylidene)cyclodeca-3,7-dien-1-ylmethanesulfonate (3a). Yield: 67%, ^{1}H NMR (400 MHz, CDCl₃) δ 5.88 (dd, J = 5.0, 2.0 Hz, 1H), 5.30 (dd, J = 11.0, 9.7 Hz, 1H), 5.15–5.07 (m, 1H), 3.01 (s, 3H), 2.58 (t, J = 3.6 Hz, 1H), 2.54 (t, J = 3.6 Hz, 1H), 2.38 (d, J = 3.4 Hz, 1H), 2.37–2.32 (m, 2H), 2.31 (t, J = 2.5 Hz, 2H), 2.30–2.25 (m, 1H), 1.72 (s, 6H), 1.58 (s, 3H), 1.56 (s, 3H). ^{13}C NMR (100 MHz, (D₆) DMSO) δ 138.25 (C-11), 137.17 (C-4), 131.69 (C-10), 129.40 (C-1), 129.24 (C-7), 120.14 (C-5), 74.64 (C-8), 39.24 (C-3), 38.65 (C-9), 38.60 (C-16), 28.82 (C-6), 25.60 (C-2), 21.42 (C-12), 21.42 (C-13), 18.81 (C-14), 16.31 (C-15). EI-MS: 299.16 [M + H⁺]. Calcd for C₁₆H₂₆O₃S (298.16): C, 64.39; H, 8.78; and O, 16.08. Found: C, 64.37; H, 8.79; and O, 16.09.

(3E,7E)-3,7-Dimethyl-10-(propan-2-ylidene)cyclodeca-3,7-dien-1-yltrifluoromethanesulfonate (3b). Yield: 64%, ^{1}H NMR (400 MHz, CDCl₃) δ 5.90–5.84 (m, 1H), 5.32 (dd, J = 11.1, 9.6 Hz, 1H), 5.13 (ddd, J = 11.7, 5.8, 4.6 Hz, 1H), 2.63 (dd, J = 13.1, 11.3 Hz, 1H), 2.55 (dd, J = 13.2, 9.4 Hz, 1H), 2.39 (dd, J = 3.0, 2.0 Hz, 1H), 2.37 (s, 1H), 2.35 (dd, J = 3.1, 2.0 Hz, 1H), 2.32 (d, J = 1.3 Hz, 1H), 2.32–2.30 (m, 1H), 2.28 (d, J = 3.7 Hz, 1H), 1.74 (s, 6H), 1.59 (s, 3H), 1.55 (s, 3H). ^{13}C NMR (100 MHz, (D₆) DMSO) δ 138.25 (C-11), 137.17 (C-4), 131.69 (C-10), 129.40 (C-1), 129.24 (C-7), 120.14 (C-5), 118.25 (C-16), 74.64 (C-8), 39.24 (C-3), 38.65 (C-9), 28.82 (C-6), 25.60 (C-2), 21.42 (C-12, C-13), 18.81 (C-14), 16.31 (C-15). EI-MS: 353.41 [M + H⁺]. Anal. calcd for C₁₆H₂₃F₃O₃S (352.13): C, 54.53; H, 6.58; F, 16.17; and O, 13.62. Found: C, 54.54; H, 6.59; F, 16.16; and O, 13.62.

(3E,7E)-3,7-Dimethyl-10-(propan-2-ylidene)cyclodeca-3,7-dien-1-yl-ethanesulfonate (3c). Yield: 61%, ^{1}H NMR (400 MHz, CDCl₃) δ 5.86 (dd, J = 5.1, 2.1 Hz, 1H), 5.30 (dd, J = 11.0, 9.7 Hz, 1H), 5.15–5.08 (m, 1H), 3.48 (q, J = 7.2 Hz, 2H), 2.58 (dd, J = 11.3, 9.2 Hz, 1H), 2.53 (dd, J = 11.3, 7.5 Hz, 1H), 2.40–2.36 (m, 1H), 2.34 (dt, J = 4.3, 1.5 Hz, 1H), 2.31 (d, J = 1.8 Hz, 1H), 2.30 (d, J = 2.2 Hz, 1H), 2.28 (dd, J = 4.5, 1.6 Hz, 1H), 2.27–2.20 (m, 1H), 1.72 (s, 6H), 1.56 (s, 3H), 1.54 (s, 3H), 1.36 (t, J = 7.1 Hz, 3H). ^{13}C NMR (100 MHz, (D₆) DMSO) δ 138.25 (C-11), 137.17 (C-4), 131.69 (C-10), 139.40 (C-1), 129.24 (C-7), 120.14 (C-5), 74.64 (C-8), 44.10 (C-16), 39.24 (C-3), 38.65 (C-9), 28.82 (C-6), 25.60 (C-2), 21.42 (C-12), 21.42 (C-13), 18.81 (C-14), 16.31 (C-15), 8.09 (C-17). EI-MS:

313.47 [M + H$^+$]. Anal. calcd for $C_{17}H_{28}O_3S$ (312.18): C, 65.35; H, 9.03; and O, 15.36. Found: C, 65.35; H, 9.01; and O, 15.36.

(3E,7E)-3,7-Dimethyl-10-(propan-2-ylidene)cyclodeca-3,7-dien-1-ylbenzenesulfonate (3d). Yield: 57%, ^{1}H NMR (400 MHz, CDCl$_3$) δ 7.77 (dd, J = 7.9, 1.4 Hz, 2H), 7.73–7.68 (m, 1H), 7.57 (t, J = 7.8 Hz, 2H), 5.85 (dd, J = 4.3, 3.0 Hz, 1H), 5.33 (dd, J = 11.0, 10.0 Hz, 1H), 5.21–5.09 (m, 1H), 2.61 (dd, J = 10.2, 8.1 Hz, 1H), 2.56 (dd, J = 10.2, 7.0 Hz, 1H), 2.43–2.40 (m, 1H), 2.40–2.36 (m, 1H), 2.35 (s, 1H), 2.35–2.33 (m, 1H), 2.33 (d, J = 1.7 Hz, 1H), 2.32–2.25 (m, 1H), 1.72 (s, 6H), 1.60 (s, 3H), 1.56 (s, 3H). ^{13}C NMR (100 MHz, (D_6) DMSO) δ 138.25 (C-11), 137.17 (C-4), 134.06 (C-16), 131.68 (C-10), 131.44 (C-19), 129.40 (C-1), 129.25 (C-18, C-20), 129.23 (C-7), 127.83 (C-17, C-21), 120.14 (C-5), 74.64 (C-8), 39.24 (C-3), 38.65 (C-9), 28.82 (C-6), 25.60 (C-2), 21.42 (C-12, C-13), 18.81 (C-14), 16.31 (C-15). EI-MS: 361.17 [M + H$^+$]. Anal. calcd for $C_{21}H_{28}O_3S$ (360.18): C, 69.96; H, 7.83; and O, 13.31. Found: C, 69.95; H, 7.85; and O, 13.32.

(3E,7E)-3,7-Dimethyl-10-(propan-2-ylidene)cyclodeca-3,7-dien-1-yl-4-methylbenzenesulfonate (3e). Yield: 62%, ^{1}H NMR (400 MHz, CDCl$_3$) δ 7.66 (d, J = 8.1 Hz, 2H), 7.35 (d, J = 7.8 Hz, 2H), 5.85 (dd, J = 4.3, 3.0 Hz, 1H), 5.33 (dd, J = 11.0, 10.0 Hz, 1H), 5.14 (ddd, J = 6.9, 5.6, 2.9 Hz, 1H), 2.61 (dd, J = 10.2, 8.1 Hz, 1H), 2.56 (dd, J = 10.2, 7.0 Hz, 1H), 2.42–2.37 (m, 2H), 2.37–2.35 (m, 2H), 2.34 (s, 3H), 2.34–2.32 (m, 1H), 2.32–2.28 (m, 1H), 1.72 (s, 6H), 1.60 (s, 3H), 1.55 (s, 3H). ^{13}C NMR (100 MHz, (D_6) DMSO) δ 144.27 (C-19), 138.25 (C-11), 137.17 (C-4), 133.84 (C-16), 131.69 (C-10), 129.93 (C-18, C-20), 129.40 (C-1), 129.24 (C-7), 128.01 (C-17, C-21), 120.14 (C-5), 74.64 (C-8), 39.24 (C-3), 38.65 (C-9), 28.82 (C-6), 25.60 (C-2), 21.42 (C-12), 21.42 (C-13), 21.26 (C-22), 18.81 (C-14), 16.31 (C-15). EI-MS: 375.54 [M + H$^+$]. Anal. calcd for $C_{22}H_{30}O_3S$ (374.19): C, 70.55; H, 8.07; and O, 12.82. Found: C, 70.55; H, 8.05; and O, 12.84.

(3E,7E)-3,7-Dimethyl-10-(propan-2-ylidene)cyclodeca-3,7-dien-1-yl-4-chlorobenzenesulfonate (3f). Yield: 52%, ^{1}H NMR (400 MHz, CDCl$_3$) δ 7.68 (d, J = 7.8 Hz, 2H), 7.63 (d, J = 8.1 Hz, 2H), 5.81 (dd, J = 5.8, 1.4 Hz, 1H), 5.32 (dd, J = 11.1, 9.8 Hz, 1H), 5.13 (ddd, J = 6.9, 5.6, 2.9 Hz, 1H), 2.63–2.57 (m, 1H), 2.54 (dd, J = 11.5, 8.1 Hz, 1H), 2.38 (dd, J = 5.3, 1.8 Hz, 1H), 2.36–2.34 (m, 1H), 2.34–2.31 (m, 2H), 2.31–2.27 (m, 1H), 2.23 (dd, J = 15.4, 1.4 Hz, 1H), 1.72 (s, 6H), 1.59 (s, 3H), 1.54 (s, 3H). ^{13}C NMR (100 MHz, (D_6) DMSO) δ 138.25 (C-11), 137.17 (C-4), 135.25 (C-19), 134.06 (C-16), 131.69 (C-10), 129.72 (C-17, C-21), 129.46 (C-18, C-20), 129.41 (C-1), 129.24 (C-4), 120.14 (C-5), 74.64 (C-8), 39.24 (C-3), 38.65 (C-9), 28.82 (C-6), 25.60 (C-2), 21.42 (C-12, C-13), 18.81 (C-14), 16.31 (C-15). EI-MS: 395.96 [M + H$^+$]. Anal. calcd for $C_{21}H_{27}ClO_3S$ (394.14): C, 63.86; H, 6.89; Cl, 8.98; and O, 12.15. Found: C, 63.85; H, 6.88; Cl, 8.99; and O, 12.15.

Cell assay

Inhibition effects of the synthesized compounds on Bel-7402, HepG2, A549 and HeLa cells were investigated according to the related ref. 19. The cells were incubated in RPMI 1640 complete culture medium consisting of 10% FBS, 100 U mL^{-1} penicillin, and 100 μg mL^{-1} streptomycin at 37 °C in a humidified atmosphere containing 5% CO$_2$. Cell growth was evaluated by MTT assay.[10] Cells were inoculated at 1.0×10^4 cells per mL

with 200 μL in each well of a 96-well plate and treated with 0–800 μmol L^{-1} of target products or 0.1% DMSO for 24 and 48 h. 20 μL of MTT was added and the mixture was incubated in the dark at 37 °C for 4 h. After the removal of MTT, cells were treated with 150 μL of DMSO. The absorbances were determined at 590 nm using an automated microplate reader (SpectraMAX190, Molecular Devices, USA).

Inhibition of c-Met kinase

The inhibition of c-Met kinase was investigated as described in a reported study.[20] The IC$_{50}$ values were determined using TR-FRET. 6 His-tagged recombinant human c-Met residues (50 nM) 974-end (Millipore) were cultured in a medium containing 2.5 mmol L^{-1} MnCl$_2$, 10 mmol L^{-1} MgCl$_2$, 20 mmol L^{-1} Tris, 2 mmol L^{-1} DTT, and 0.01% Tween 20 with 5 mmol L^{-1} ATP and 200 nmol L^{-1} 5FAM-KKK-SPGEYVNIGFG-NH$_2$ at room temperature for 60 min. Compounds were tested with increasing concentrations. Reactions were terminated using IMAP stop solution. Plates were incubated overnight and analyzed using AiphaQuest.

Molecular docking

Molecular docking was performed according to the related ref. 11. The docking experiment was carried out using the CDocker program, which was connected with the Accelrys Discovery Studio 2.5.5. The programs were adapted with an empirical scoring function and a patented search engine.[21,22] Briefly, ligands were docked into the corresponding protein's binding site in compliance with the protocol, which was generated by ligands from the crystal structure of 3DKC with random hydrogen atoms and Gasteiger–Hückel charges, but not water. The ligands' other parameters were default values except that the threshold was 1. The structure of the receptor was minimized to 10 000 cycles using the Powell method in DS 2.5.5. The geometries of all compounds were optimized by the conjugate gradient method of TRIPOS. The convergence criterion was identified as 0.001 kcal mol^{-1}.

MD simulations

The MD simulations were performed on the basis of molecular docking using AMBER 10.0 for ligands and AMBER ff03 for proteins. The Gaussian 03 program was used to calculate partial atomic charges at a neutral pH, with histidines 164 and 200 protonated at the δ position. The SHAKE algorithm was used to restrict all the bonds, given the time step of 2 fs and cut-off distance of 8 Å, with long-range electrostatic interactions treated with the particle mesh Ewald (PME) method.[23,24] The heating operation was carried out from 0 to 300 K in 50 ps using Langevin dynamics at a constant volume and equilibrated for 100 ps at a constant pressure of 1 atm after four steps of minimizations, which included 2500 cycles of steepest descent minimization, followed by 2500 cycles of conjugated gradient minimization. Heavy atoms of the receptor–ligand complex were restrained to 0, 10, 100, and 500 kcal (mol^{-1} Å^2) and were 10 kcal (mol^{-1} Å^2) during the heating and equilibration steps, whereas solvent molecules were not restricted. Finally, periodic boundary conditions of 8 ns were employed for the whole

system with a normal pressure of 1 atm and normal temperature of 300 K in the production step.

MM-PBSA estimation of binding free energy ΔG_{pred}

For each system, ΔG_{pred} values were calculated using 100 snapshots from the last 1 ns trajectory with an interval of 10 ps by the molecular mechanics Poisson–Boltzmann surface area (MM-PBSA) method.[25–28]

Results and discussion

Chemistry

The target compounds **2** and **3a–3f** were synthesized, as described in Fig. 3. Different sulfonic acids reacted with (3*E*,7*E*)-3,7-dimethyl-10-(propan-2-ylidene) cyclodeca-3,7-dienol (**2**) to obtain (3*E*,7*E*)-3,7-dimethyl-10-(propan-2-ylidene) cyclodeca-3,7-dien-1-ylmethanesulfonate (**3a**), (3*E*,7*E*)-3,7-dimethyl-10-(propan-2-ylidene)cyclodeca-3,7-dien-1-yltrifluoromethanesulfonate (**3b**), (3*E*,7*E*)-3,7-dimethyl-10-(propan-2-ylidene)cyclodeca-3,7-dien-1-ylethanesulfonate (**3c**), (3*E*,7*E*)-3,7-dimethyl-10-(propan-2-ylidene)cyclodeca-3,7-dien-1-yl-benzenesulfonate (**3d**), and (3*E*,7*E*)-3,7-dimethyl-10-(propan-2-ylidene)cyclodeca-3,7-dien-1-yl-4-chlorobenzene sulfonate (**3f**) *via* acyl chloride esterification reaction with yields of 67%, 61%, 64%, 57%, and 52%, respectively. The esterification reaction provided good yields using dry THF as a solvent and pyridine as an acid-binding agent. The residual target compounds (3*E*,7*E*)-3,7-dimethyl-10-(propan-2-ylidene)cyclodeca-3,7-dien-1-yl-4-methylbenzenesulfonate (**3e**) were obtained *via* a DMAP/DCC esterification reaction with a yield of 62%. This reaction was carried out using dry DCM or acetonitrile as a solvent, DMAP as a catalyst, and DCC as a dehydrator and can be widely applied.

Due to the distinct difference in polarity, compounds could be easily separated. Structural modification of germacrone and a systematic study showed that 8-hydroxyl group may require further optimization studies and a range of substituents could be suitable for this position.

Evaluation of biological activity

Biological activities were investigated by checking the effect of germacrone and its derivatives on the growth of Bel-7402 cells, HepG2 cells, A549, and HeLa cells. These cells were treated with germacrone and its derivatives at the concentrations of 12.5 μmol L^{-1}, 25 μmol L^{-1}, 50 μmol L^{-1}, 100 μmol L^{-1}, 200 μmol L^{-1}, 400 μmol L^{-1}, and 800 μmol L^{-1}, respectively. An MTT assay was then applied at 24 h and 48 h. As shown in Table 1, the proliferations of HepG2, Bel7402, A549, and Hela cells were inhibited in a dose-dependent manner, and the cytolytic activity was markedly inhibited at the same time. Moreover, the IC$_{50}$ values of germacrone against Bel-7402 cells, HepG2 cells, A549, and HeLa cells were about 173.54 μM, 169.52 μM, 179.97 μM, and 160.69 μM. The growth-inhibitory effect had no significant differences after incubation with germacrone and derivatives for 24 h and 48 h (Fig. 4); thus, there was no significant influence on the antiproliferation effect of compounds on Bel-7402 cells, HepG2 cells, A549, and HeLa cells with an extended treatment time after 24 h. This might be caused by the saturation of intracellular drug concentration within 24 hours. Compounds **3e** and **3f**, in which R was substituted with benzene, showed high inhibition and **3e** showed highest activity against HepG2 with an IC$_{50}$ value of 56.22
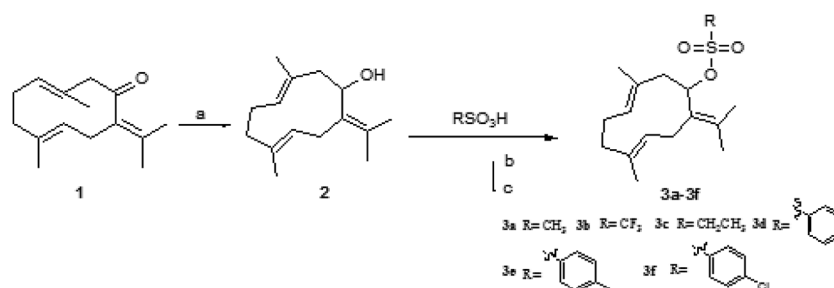

Fig. 3 Synthesis of **3a–3f** reagents and conditions: (a) LiAlH$_4$, THF, r.t., 1 h; (b) SOCl$_2$, DMF, Py, THF, r.t., 4 h; and (c) DMAP, DCC, r.t., 24 h.

Table 1 IC$_{50}$ values of compounds for Bel-7402, HepG2, A549, and Hela cells

| Compound	Bel-7402 IC$_{50}$ (μM)		HepG2 IC$_{50}$ (μM)		A549 IC$_{50}$ (μM)		HeLa IC$_{50}$ (μM)	
	24 h	48 h	24 h	48 h	24 h	48 h	24 h	48 h
1	173.54	177.21	169.52	174.56	179.97	177.21	160.69	167.78
2	167.08	166.32	155.20	161.54	177.21	185.24	157.31	163.15
3a	122.23	125.68	119.09	121.08	127.68	131.45	125.96	129.44
3b	88.87	92.44	79.98	77.80	97.74	95.52	100.25	97.28
3c	105.05	110.14	98.54	95.65	111.28	115.69	108.97	105.88
3d	92.00	91.02	84.67	87.74	101.35	97.74	102.80	108.36
3e	71.78	74.68	56.22	57.18	84.47	81.00	88.64	89.26
3f	77.04	79.45	64.12	62.99	91.25	95.65	95.24	99.11
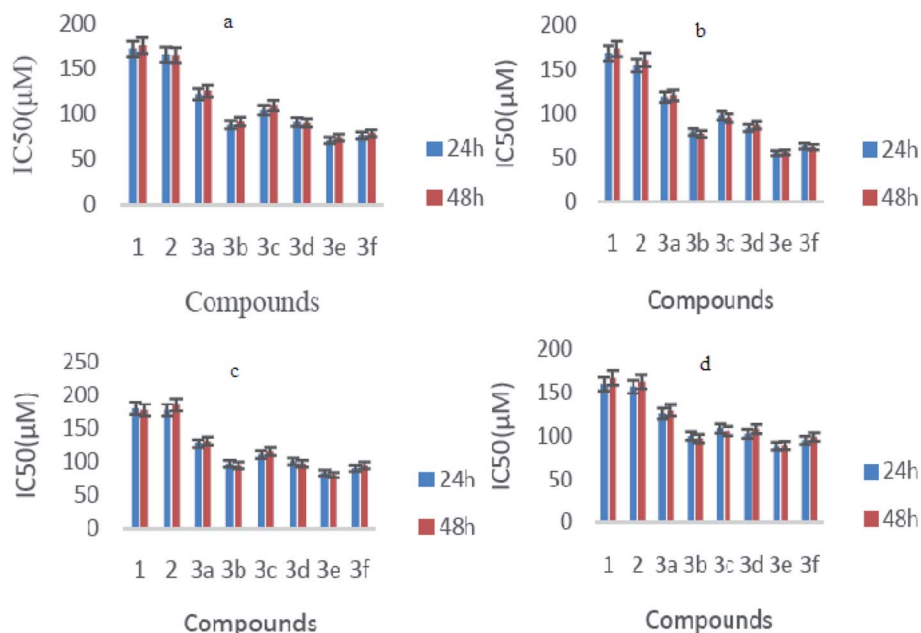
Fig. 4   Inhibition of germacrone derivatives on Bel-7402, HepG2, A549, and HeLa cells. (a) The effect of compounds on Bel-7402 cells. (b) The effect of compounds on HepG2 cells. (c) The effect of compounds on A549 cells. (d) The effect of compounds on HeLa cells.

μM. The results of inhibition on c-Met showed that these derivatives exhibited a stronger inhibitory effect than germacrone (Fig. 5). Since the results suggested that the derivatives have good activity, we could initially confirm that the designed compounds might be well worth investigation on the basis of molecular docking, molecular dynamics simulations, and preliminary activity tests. In conclusion, our strategy to design germacrone derivatives was successful in obtaining the desired compounds, which demonstrated a stronger inhibitory effect on cancer cells and c-Met kinase. These compounds might be useful as lead structures for the development of anti-cancer agents, and this study could supply important information for building a chemical library and the basis for further research.

Docking studies

In our previous study, we performed docking studies using several PDB proteins including 3DKF, 2WGJ, 2RFS, and 3DKC, in which only 3DKC interacted with germacrone and its

derivatives owing to sesquiterpene structures of these compounds; therefore, we chose this compound to perform the docking experiments. The 3DKC is the crystal structure of c-Met kinase in complex with ATP and its details can be obtained from http://www.rcsb.org/pdb/explore/materialsAndMethods.do?structureId=3DKC, which is widely used.[29–31]

Molecular docking suggested that these compounds were bound to the active site of the protein 3DKC (shown in Fig. 6). The binding energies of the complexes between each compound (1–3f) and the active site of the receptor are shown in Table 2. The binding energies were higher when R was a benzene ring and the compounds showed higher inhibition, of which a substituted benzene ring had stronger binding energies and inhibition. The interaction between the (E,E)-1,5-cyclodecadiene system and the protein crystal 3DKC seems to be strong, and the binding forces were mainly hydrophobic forces, whereas another clear interaction was the σ–π interaction
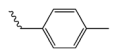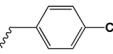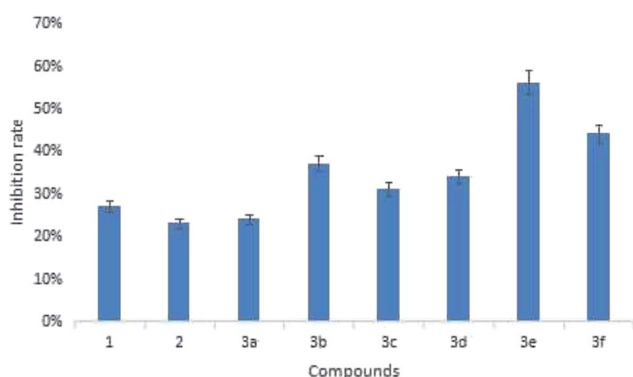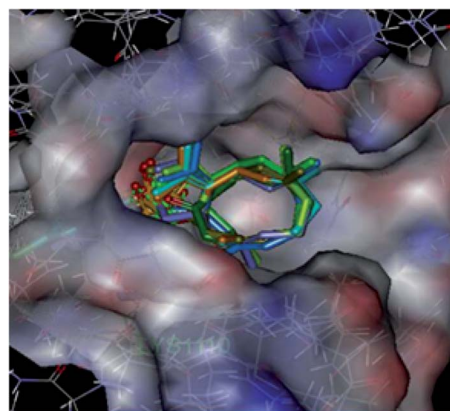

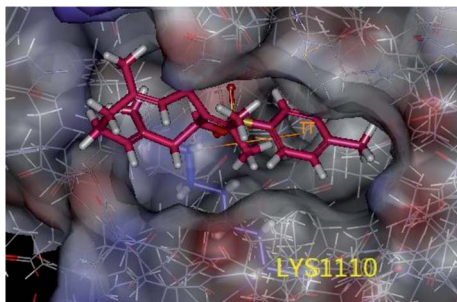Fig. 5   Inhibition of compounds on c-Met Kinase.

Fig. 6   Compact binding modes of all compounds (PDB code: 3DKC).

Table 2 Binding energies of complexes between compounds and 3DKC

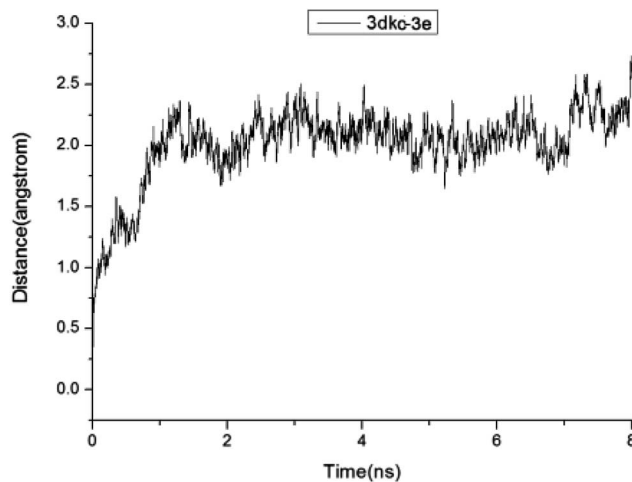| Compounds	R	c-Met inhibition rate (%)	−CDOCKER energy (kcal mol^{-1})
1	—	27%	29.4387
2	−OH	23%	22.0488
3a	Me	24%	22.7005
3b	−CF$_3$	37%	42.2213
3c	−CH$_2$CH$_3$	31%	32.4854
3d	Ph	34%	38.7086
3e	〰〜⟨benzene ring with CH$_3$⟩	56%	65.5007
3f	〰〜⟨benzene ring with Cl⟩	44%	47.4545

Fig. 7 Conformations of **3e**.

between the benzene ring with LYS1110 and GLY1087. Compound **3e** showed the highest activity owing to the π–π stacking interaction of the benzene ring and hydrophobic interaction of methyl, as shown in Fig. 7.

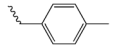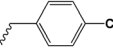### MD simulations and ΔG$_{pred}$ calculation

Building on the structural data from diverse experimental sources, today's MD simulations permit the exploration of biological processes in an unparalleled detail. Since molecular docking studies reported a probably momentary binding mode, which might be unreasonable and unstable, molecular dynamics simulations were applied to carry out further research of the binding stabilities between the compounds (**1–3f**) and 3DKC.

The crystal structures of the 3DKC complex with **1–3f** were used to investigate the reliability of molecular dynamics simulations. The root mean square deviation (RMSD) curve and the surface area curve of the 1 ns MD simulation indicated that the structure of **3e** was in a relatively stable state after 1 ns and the MD trajectories were quite smooth (shown in Fig. 8), whereas other compounds were unstable with uneven MD trajectories (as shown in ESI†). The MD parameters were suitable for the MD simulations.

Given identical MD conditions, the two 3DKC–ligand complexes were used to perform the molecular dynamics simulations for eight nanoseconds. The RMSD curves of all compounds were stable during the MD simulations. In the

Fig. 8 Plots of RMSD for all of the backbone atoms (Å) *vs.* simulation time (ns) for 3DKC in complex with **3e**.

Table 3 The value of −CDOCKER energy

Compounds	R	c-Met inhibition rate (%)	ΔG$_{pred}$ energy (kcal mol^{-1})
1	—	27%	16.35
2	−OH	23%	12.31
3a	Me	24%	12.48
3b	−CF$_3$	37%	21.09
3c	−CH$_2$CH$_3$	31%	20.11
3d	Ph	34%	20.23
3e	〰〜⟨benzene ring with CH$_3$⟩	56%	28.36
3f	〰〜⟨benzene ring with Cl⟩	44%	25.41

experiment, ΔG$_{pred}$ values of less than −25 kcal mol^{-1} were selected and used to evaluate 3DKC inhibitory activity. The predicted ΔG$_{pred}$ value of **3e** is −28.36 kcal mol^{-1}, whereas the predicted ΔG$_{pred}$ values of other compounds were more than −25 kcal mol^{-1} (shown in Table 3). To save the computational time and reduce the computational cost of the MD-based screening studies, we did not consider the entropy contribution because of the extremely time-consuming nature of the normal mode calculation of entropy for large systems. Therefore, the calculated ΔG$_{pred}$ values in the present study were inadequate owing to the omission of entropy contribution.

Conclusions

This study designed and synthesized novel bioactivity compounds using the natural product germacrone as the lead compound based on the design theory of alkylating agents. The results showed that the majority of compounds had moderate inhibition on cancer cells and c-Met kinase. These compounds can be further studied as antitumor lead structures to lay the foundation for developing anticancer compounds with clinical value. The results of molecular docking and molecular

dynamics simulations were very important in explaining the molecular mechanism of eminent activities to c-Met kinase and binding stabilities between the compounds and their receptors. Moreover, these results can provide a theoretical basis for further research on c-Met inhibitors.

Acknowledgements

References

1 W. Chen, Y. Liu, M. Gao, J. Wu, A. Wang and R. Shi, Antiangiogenesis effect of essential oil from *Curcuma zedoaria in vitro* and *in vivo*, *J. Ethnopharmacol.*, 2011, **133**(1), 220–226.

2 C. Chen, Y. Chen, Y. His, *et al.* Chemical Constituents and Anticancer Activity of *Curcuma zedoaria* Roscoe Essential Oil against Non-Small Cell Lung Carcinoma Cells *in Vitro* and *in Vivo*, *J. Agric. Food Chem.*, 2013, **61**(47), 11418–11427.

3 W. Seo, J. Hwang, S. Kang, *et al.* Suppressive effect of *Zedoariae rhizoma* on pulmonary metastasis of B16 melanoma cells, *J. Ethnopharmacol.*, 2005, **101**(3), 249–257.

4 N. Dde, M. Souza, R. Neto, *et al.* Phytochemical analysis and analgesic properties of *Curcuma zedoaria* grown in Brazil, *Phytomedicine*, 2002, **9**(5), 427–432.

5 B. Wilson, J. Abraham, V. Manju, *et al.* Antimicrobial activity of *Curcuma zedoaria* and *Curcuma malabarica* tubers, *J. Ethnopharmacol.*, 2005, **99**(1), 147–151.

6 H. Matsuda, S. Tewtrakul, T. Morikawa, A. Nakamura and M. Yoshikawa, Antiallergic principles from Thai zedoary: structural requirements of curcuminoids for inhibition of degranulation and effect on the release of TNF-α and IL-4 in RBL-2H3 cells, *Bioorg. Med. Chem.*, 2004, **12**(22), 5891–5898.

7 Y. Dang, X. Li, Q. Zhang and Y. Wang, Preparative isolation and purification of six volatile compounds from essential oil of *Curcuma wenyujin* using high-performance centrifugal partition chromatography, *J. Sep. Sci.*, 2010, **33**(11), 1658–1664.

8 W. Cho, J. Nam, H. Kang, *et al.* Zedoarondiol isolated from the rhizome of *Curcuma heyneana* is involved in the inhibition of iNOS, COX-2 and pro-inflammatory cytokines *via* the downregulation of NF-kappa B pathway in LPS-stimulated murine macrophages, *Int. Immunopharmacol.*, 2009, **9**(9), 1049–1057.

9 X. Xiao, Y. Zhao, H. Yuan, *et al.* Study on the effect of *Rhizoma curcuma* Longa on gastrin receptor, *J. Chin. Mater. Med.*, 2002, **25**(3), 184–185.

10 Y. Liu, W. Wang, B. Fang, *et al.* Anti-tumor effect of germacrone on human hepatoma cell lines through inducing G2/M cell cycle arrest and promoting apoptosis, *Eur. J. Pharmacol.*, 2013, **698**(2), 95–102.

11 L. Ye, Y. Tian, Z. Li, *et al.* Design, synthesis and molecular docking studies of some novel spiro[indoline-3,4′-piperidine]-2(1*H*)-ones as potential c-Met inhibitors, *Eur. J. Med. Chem.*, 2012, **50**, 370–375.

12 P. Ma, T. Kijima, G. Maulik, *et al.* c-Met mutational analysis in small cell lung cancer: novel juxtamembrane domain mutations regulating cytoskeletal functions, *Cancer Res.*, 2003, **63**(19), 6272–6281.

13 P. Ma, S. Jagadeesh, R. Jagadeeswaran, *et al.* c-Met expression/activation, functions, and mutations in non-small cell lung cancer, *Proc. Am. Assoc. Canc. Res.*, 2004, **45**, 1875.

14 D. Renzo, M. Olivero, T. Martone, *et al.* Somatic mutations of the MET oncogene are selected during metastatic spread of human HNSC carcinomas, *Oncogene*, 2000, **19**(12), 1547–1555.

15 J. Lee, S. Han, H. Cho, *et al.* A novel germ line juxtamembrane Met mutation in human gastric cancer, *Oncogene*, 2000, **19**(43), 4947–4953.

16 F. Yang, S. Praveena and C. Patrick, Met signaling: novel targeted inhibition and its clinical development in lung cancer, *J. Thorac. Oncol.*, 2012, **7**(2), 459–467.

17 M. Li, P. Yang, Y. Liu, *et al.* Low c-Met expression levels are prognostic for and predict the benefits of temozolomide chemotherapy in malignant gliomas, *Sci. Rep.*, 2016, **6**, 1–10.

18 T. L. Lemke, D. A. Williams and V. F. Roche, *et al.*, *Foye's principles of medicinal chemistry*, Wolters Kluwer: Lippincott William and Wilkins, 7th edn, 2013.

19 W. Chen, Y. Liu, M. Li, *et al.* Anti-tumor effect of α-pinene on human hepatoma cell lines through inducing G2/M cell cycle arrest, *J. Pharmacol. Sci.*, 2015, **3**, 332–338.

20 J. Porter, S. Lumb, R. Franklin, *et al.* Discovery of 4-azaindoles as novel inhibitors of c-Met kinase, *Bioorg. Med. Chem. Lett.*, 2009, **19**(10), 2780–2784.

21 A. Jain, Surflex: fully automatic flexible molecular docking using a molecular similarity-based search engine, *J. Med. Chem.*, 2003, **46**(4), 499–511.

22 A. Jain, Surflex-Dock2.1: robust performance from ligand energetic modeling, ring flexibility, and knowledge-based search, *J. Comput.–Aided Mol. Des.*, 2007, **21**(5), 281–306.

23 Z. Li, Y. Cai, Y. Cheng, *et al.* Identification of Novel Phosphodiesterase-4D Inhibitors Prescreened by Molecular Dynamics Augmented Modeling and Validated by Bioassay, *J. Chem. Inf. Model.*, 2013, **53**(4), 972–981.

24 M. Shuichi and P. Kollman, Settle: An analytical version of the SHAKE and RATTLE algorithm for rigid water models, *J. Comput. Chem.*, 1992, **13**(8), 952–962.

25 I. Massova and P. Kollman, Combined molecular mechanical and continuum solvent approach (MM-PBSA/GBSA) to predict ligand binding, *Perspect. Drug Discovery Des.*, 2000, **18**(1), 113–135.

26 T. Hou, J. Wang, Y. Li and W. Wang, Assessing the performance of the MM/PBSA and MM/GBSA methods. 1. The accuracy of binding free energy calculations based on molecular dynamics simulations, *J. Chem. Inf. Model.*, 2011, **51**(1), 69–82.

27 M. Liu, M. Yuan, M. Luo, *et al.* Binding of curcumin with glyoxalase I: molecular docking, molecular dynamics simulations, and kinetics analysis, *Biophys. Chem.*, 2010, **147**(1–2), 28–34.

28 L. He, F. He, H. Bi, *et al.* Isoform-selective inhibition of chrysin towards human cytochrome P450 1A2. Kinetics analysis, molecular docking, and molecular dynamics simulations, *Bioorg. Med. Chem. Lett.*, 2010, **20**(20), 6008–6012.

29 S. G. Buchanan, J. Hendle, P. S. Lee, *et al.* SGX523 is an exquisitely selective, ATP-competitive inhibitor of the MET receptor tyrosine kinase with antitumor activity *in vivo*, *Mol. Cancer Ther.*, 2009, **8**(12), 3181–3190.

30 J. G. Christensen, R. J. Schreck, P. Kuruganti, *et al.* A selective small molecule inhibitor of c-Met kinase inhibits c-Met-dependent phenotypes *in vitro* and exhibits cytoreductive antitumor activity in vivo, *Cancer Res.*, 2003, **63**(21), 7345.

31 L. Wang, J. Ai, Y. Shen, *et al.* SOMCL-863, a novel, selective and orally bioavailable small-molecule c-Met inhibitor, exhibits antitumor activity both *in vitro*, and *in vivo*, *Cancer Lett.*, 2014, **351**(1), 143–150.